Full length article

Methylmercury-induced developmental toxicity is associated with oxidative stress and cofilin phosphorylation. Cellular and human studies

Beatriz Caballero[a,b,1], Nair Olguin[a,b,1], Francisco Campos[a,b,2], Marcelo Farina[a,c], Ferran Ballester[b,d], Maria-Jose Lopez-Espinosa[b,d], Sabrina Llop[b,d], Eduard Rodríguez-Farré[a,b], Cristina Suñol[a,b,*]

[a] Institut d'Investigacions Biomèdiques de Barcelona, Consejo Superior de Investigaciones Científicas (IIBB-CSIC), Institut d'Investigacions Biomèdiques August Pi i Sunyer (IDIBAPS), Barcelona, Spain
[b] CIBER Epidemiología y Salud Pública (CIBERESP), Spain
[c] Departamento de Bioquímica, Centro de Ciências Biológicas, Universidade Federal de Santa Catarina, Florianópolis, Santa Catarina, Brazil
[d] Epidemiology and Environmental Health Joint Research Unit, FISABIO – Universitat Jaume I – Universitat de València, Valencia, Spain

A B S T R A C T

Environmental exposure to methylmercury (MeHg) during development is of concern because it is easily incorporated in children's body both pre- and post-natal, it acts at several levels of neural pathways (mitochondria, cytoskeleton, neurotransmission) and it causes behavioral impairment in child. We evaluated the effects of prolonged exposure to 10–600 nM MeHg on primary cultures of mouse cortical (CCN) and of cerebellar granule cells (CGC) during their differentiation period. In addition, it was studied if prenatal MeHg exposure correlated with altered antioxidant defenses and cofilin phosphorylation in human placentas (n = 12) from the INMA cohort (Spain).

Exposure to MeHg for 9 days in vitro (DIV) resulted in protein carbonylation and in cell death at concentrations ≥ 200 nM and ≥ 300 nM, respectively. Exposure of CCN and CGC to non-cytotoxic MeHg concentrations for 5 DIV induced an early concentration-dependent decrease in cofilin phosphorylation. Furthermore, in both cell types actin was translocated from the cytosol to the mitochondria whereas cofilin translocation was found only in CGC. Translocation of cofilin and actin to mitochondria in CGC occurred from 30 nM MeHg onwards. We also found an increased expression of cortactin and LIMK1 mRNA in CGC but not in CCN. All these effects were prevented by the antioxidant probucol.

Cofilin phosphorylation was significantly decreased and a trend for decreased activity of glutathione reductase and glutathione peroxidase was found in the fetal side of human placental samples from the highest (20–40 μg/L) MeHg-exposed group when compared with the low (<7 μg/L) MeHg-exposed group.

In summary, cofilin dephosphorylation and oxidative stress are hallmarks of MeHg exposure in both experimental and human systems.

© 2016 Elsevier B.V. All rights reserved.

1. Introduction

Methylmercury (MeHg), a relevant persistent environmental contaminant, is widely recognized as a potent neurotoxicant in humans (WHO, 2007) since it may affect both the developing and the mature central nervous systems (CNS). Ingestion of contaminated fish is the primary source of MeHg exposure (Mergler et al., 2007; Ramon et al., 2011; Vieira et al., 2015; Xu and Newman, 2015) and both developmental and aging states are thought to exacerbate the neurotoxic effects of this organometal with primary signs of neurological dysfunction. In highly exposed populations

* Corresponding author at: Department of Neurochemistry and Neuropharmacology, Institut d'Investigacions Biomèdiques de Barcelona, Consejo Superior de Investigaciones Científicas, IIBB-CSIC-IDIBAPS, Rosselló 161, E-08036 Barcelona, Spain.
  E-mail address: csenqi@iibb.csic.es (C. Suñol).
[1] These authors equally contributed to the work.
[2] Current address: Clinical Neurosciences Research Laboratory, Department of Neurology, Hospital Clínico Universitario, Health Research Institute of Santiago de Compostela (IDIS), University of Santiago de Compostela, Santiago de Compostela, Spain.

these signs include cerebellar ataxia, constriction of the visual fields and sensory disturbances as it was observed in patients affected by the Minamata disease (Ekino et al., 2007). The most susceptible cerebral regions to MeHg-mediated injury are the cerebellum, more specifically the cerebellar granule cells (CGC), the calcarine area and the postcentral gyrus whereas no-significant differences are found in the white matter of the corpus callosum (Korogi et al., 1994; Sanfeliu et al., 2003). At the intracellular level MeHg-induced cytotoxicity in neurons has been ascribed to three major mechanisms: perturbation of intracellular Ca^{+2} levels, generation of oxidative stress and interactions with critical sulphydryl groups (Castoldi et al., 2001; Do Nascimento et al., 2008). More recently, the interaction of MeHg with seleno amino acids has been reported (Farina et al., 2009; Khan and Wang, 2009). Hallmarks of MeHg neurotoxicity in experimental *in vivo* and *in vitro* models include apoptosis, inhibition of protein synthesis, microtubule disruption or depolymerization and disturbance of neurotransmission (Yoshino et al., 1966; Castoldi et al., 2000, 2001; Dare et al., 2000, 2001; Fonfría et al., 2001, 2005; Ceccatelli et al., 2010; Hogberg et al., 2010).

One of the main intracellular targets for MeHg neurotoxicity is the mitochondrion (Castoldi et al., 2001), where this organometal is early accumulated in the brain following its administration (Yoshino et al., 1966). This accumulation has been associated to changes in mitochondrial morphology in the developing rat brain (O'Kusky 1983) and loss of the mitochondrial membrane potential (Castoldi et al., 2000). Likewise, mitochondria and cytoskeletal alterations such as neurite degeneration and neuronal network fragmentation have been reported to occur preceding MeHg-induced apoptosis in cultured cerebral cortical neurons (CCN) (Fujimura et al., 2009) and CGC neurons (Castoldi et al., 2000; Vendrell et al., 2007, 2010). In this way, cofilin, a cytoskeletal protein member of the actin depolymerizing factor (ADF), was previously found in mitochondrial fractions after exposure to MeHg in cultured CGC (Vendrell et al., 2010). Cofilin is a low-molecular weight cytosolic protein ubiquitously expressed which is present in both phosphorylated (P-cofilin) and non-phosphorylated states (non-P-cofilin). This protein regulates actin dynamics by promoting the depolymerization and severing of actin filaments, and regulating the recycling of the resulting monomers (Gourlay and Ayscough, 2005). Thus, the balance between non-P-cofilin and P-cofilin facilitates actin filament turnover whose dynamics and reorganization are responsible for key events modulating neuron survival such as neuron shape and polarity, as well as dendrite spine physiology including spine formation and maintenance, receptor trafficking and synaptic plasticity (Spence and Soderling, 2015). There is also a redox regulation of cofilin via its four cysteine residues; in fact, cofilin oxidation has been reported in different cell types and under different oxidative conditions (reviewed by Samstag et al., 2013). Also, it has been suggested that cofilin has an important function during the initiation phase of apoptosis, being the mitochondrial transloca-tion of cofilin an essential step for engaging the apoptotic pathway (Chua et al., 2003; Li et al., 2013). In this sense, Samstag et al. (2013) have identified that cofilin oxidation is the molecular switch that targets cofilin to the mitochondria in T-cells. Furthermore, mitochondrial association of cofilin during apoptosis is preceded by actin, which translocates to mitochondria during apoptotic cell death. On the other hand, dephosphorylated cofilin (Ser 3) is the cofilin form that is translocated to mitochondria (Li et al., 2015b). In previous works, we described that primary cultures of CGC showed a reduction of P-cofilin in response to MeHg exposure along with increased levels of non-P-cofilin in mitochondrial fractions (Vendrell et al., 2010).

Moreover, MeHg can lead to the generation of oxidative stress through interaction with selenol and thiol groups, as pointed out above. Therefore, it is probable that, in addition to bind to specific thiol-containing proteins, MeHg can also bind in a stable way to selenoproteins, such as antioxidant enzymes, glutathione peroxidase (GPx) and thioredoxin reductase (TrxR) (Farina et al., 2011). These proteins are important components of the cellular antioxidant system, and their inhibition contributes to the disruption of the normal redox balance of brain cells. According to this, it has been proposed that antioxidants such as propyl gallate and probucol (PB) may be used as neuroprotective agents (Gassó et al., 2001). In fact, the beneficial effects of PB have been found to be correlated with increased GPx-1 activity and decreased lipid peroxidation (Farina et al., 2009).

In the present work, we have further investigated the intracellular changes in P-cofilin and cofilin/actin localization after long-term exposure to low MeHg concentrations by using an *in vitro* paradigm that compares two cell types differentially affected by MeHg: mice CGC and CCN. After confirming that MeHg induced cofilin dephosphorylation and oxidative stress in both cell types we studied these variables in human placentas from individuals with known MeHg exposure since this tissue mediates the transfer of mercury from mothers to fetuses during the gestational period.

2. Experimental procedures

2.1. Materials

Pregnant NMRI mice (16th day of gestation) and 7-day-old NMRI mice were obtained from Charles River, Iffa Credo (St. Germain-sur-l'Arbreste, France). Dulbecco's modified Minimum Essential Medium (DMEM) was from Biochrom (Berlin, Germany). Rabbit polyclonal IgG anti-cofilin 1 and anti-Ser 3 P-cofilin 1 were from Santa Cruz Biotechnology (Santa Cruz, CA). Monoclonal anti-β actin primary antibody was from Sigma (St. Louis, MO) and protein A/G-horseradish peroxidase-conjugated secondary antibody was from Jackson Laboratories (Baltimore, USA). Protein carbonyl enzyme immuno-assay kit (BIOCELL PC TEST) was from BioCell Corporation Ltd. (Auckland, NZ). MeHg was from ICN (Cleveland, Ohio, USA). Any others reagents including jasplakinolide (JAS) were also purchased from Sigma Chemical Co. (St. Louis, MO, USA).

Human placentas belonged to participants from the INMA-Valencia mother-infant cohort (Spain) (Childhood and Environment; www.proyectoinma.org). Placenta samples were collected at delivery in 2004, and pieces of maternal and fetal sides were immediately dissected, coded, frozen and stored confidentially and anonymously at −80 °C until processed. A subset of 12 placental samples was selected as function of the total mercury concentrations measured in cord blood (low exposure (<7 µg/L) and high exposure (20–40 µg/L)). Informed consent was obtained from all participants and the study was approved by the Hospital La Fe Ethics Committee (Valencia, Spain).

2.2. Neuronal cell culture

Primary cultures were prepared as previously described (Farina et al., 2009; Vendrell et al., 2010; Regueiro et al., 2015). Both CGC and CCN cells were seeded (1.6×10^6 cells/mL, except otherwise stated) on multi-well-plates precoated with poly-D-lysine and incubated in a modified DMEM solution (31 mM glucose and 0.2 mM glutamine), supplemented with insulin, penicillin and 10% foetal calf serum, containing 5 mM KCl for CCN and 25 mM KCl for CGC in a humidified 5% CO2/95% air atmosphere at 37 °C without changing the culture medium, unless otherwise specified. A mixture of 5 µM 5-fluoro-2′-deoxyuridine and 20 µM uridine was added to the cultures after 24 h incubation to prevent glial

proliferation. Animals were handled in compliance with protocols approved by the Generalitat de Catalunya, Spain, following European Union Guidelines.

2.3. Cell treatments

Cells seeded in 96 multi-well plates were used for viability assays and in 6-well plates for obtaining protein samples used in western blotting. Cells seeded in 6-well plates were also isolated for RNA extraction. Cultured CGC and CCN were exposed to MeHg (0–600 nM) in the absence and the presence of 10 μM PB by adding concentrated solutions of these compounds directly to the culture medium at 24 h after seeding (day *in vitro* (DIV) 1), and kept in the same medium up to 5–9 DIV. We selected these concentration range and exposure time based on our previous work where 300 nM MeHg induces less than 10% cell death in CGC exposed for 5 DIV but about 50% cell death after 11 DIV (Farina et al., 2009; Vendrell et al., 2010). Cell viability and protein oxidation were determined at the longer exposure time (from DIV 1 to DIV 9) whereas cofilin dynamics were earlier determined (at DIV 5) under conditions of MeHg exposure that did not produce appreciable cytotoxicity. When cells were treated with the antioxidant PB, both MeHg and PB were simultaneous added. PB was dissolved in dimethylsulfoxide (DMSO), which final concentration did not exceed 0.1% in the culture medium. MeHg was dissolved in deionized water. MeHg solutions were handled in compliance of safety measures for toxic chemicals. Excess solutions were withdrawn as specific metal disposals. Additionally, cultured CGC and CCN were exposed to 100 nM jasplakinolide (JAS) by adding concentrated solutions of this compound directly to the culture medium at DIV 1 and for 15 min. Then, the medium containing JAS was replaced by medium containing different MeHg concentrations (0–600 nM). JAS was also dissolved in DMSO, whose concentration did not exceed 0.1% in the culture medium.

2.4. Cell viability assays

Cell viability was first assessed by visual inspection under phase-contrast microscopy and then by the MTT assay, which is based on the reduction by viable cells of 3-(4,5-dimethythiazol-2-yl)-2,5-diphenyl-tetrazolium bromide (MTT) to a formazan product via a group of nonspecific mitochondrial dehydrogenases as previously described (Regueiro et al., 2015). Absorbance was measured at 570 nm with background subtraction. Cell viability was expressed as a percentage of the controls. Cell viability in cells continuously exposed to probucol was determined by measuring the uptake of propidium iodide (PI), which is excluded by living cells but rapidly enters cells with damaged membranes and binds to DNA, rendering them brightly fluorescent, as previously described (Farina et al., 2009). PI uptake values were expressed as arbitrary fluorescence units.

2.5. ELISA of carbonyl proteins

Protein carbonyl was determined colorimetrically at 450 nm following manufacturer's instructions from protein carbonyl enzyme immuno-assay kit (BIOCELL PC TEST). Briefly, protein samples (20 μg) were derivatized with dinitro-phenylhydrazine (DNP) and then non-specifically adsorbed to an ELISA plate. Free DNP and non-protein constituents are easily washed away, giving minimal interference. The adsorbed proteins bind to biotinylated anti-DNP antibody followed by streptavidin-biotinylated horse-radish peroxidase. Absorbances were related to a standard curve prepared from serum albumin containing increasing proportions of hypochlorous acid-oxidized protein. Results were expressed as nmol of protein carbonyl/mg of protein (% with respect to control).

2.6. Preparation of cytosolic and mitochondrial cell extracts

At the end of the exposure period, primary cultures were rinsed with cold PBS, and incubated 15 min on ice with the CelLytic MTM mammalian lysis reagent, then the cells were scraped to increase total protein yield. To obtain mitochondrial-enriched fractions, collected cells were homogenized in a Dounce Teflon-glass homogenizer (30 passes; 450 rpm) and submitted to differential centrifugations. Supernatants obtained after centrifugation at 800 x g for 10 min were re-centrifuged at 14,000 x g for 30 min at 4 °C. The supernatant obtained was the cytosolic-enriched fractions and the final pellet, containing the mitochondrial-enriched fractions, was re-suspended in 50 μl of CelLytic buffer. Finally, cytosolic and mitochondrial extracts were sonicated with 3 ultrasonic bursts of 30 s each with sample, cooled immediately on ice and stored at −80 °C until use. Protein content was quantified by the Bradford method.

2.7. Preparation of total placental extracts

For western blotting assays, placenta samples were thawed, rinsed with 0.9% NaCl, homogenized (80 mg tissue/mL) with lysis buffer (50 mM Tris-HCl, 150 mM NaCl, 0.1% SDS, 1% NP-40 and protease inhibitors), boiled at 100 °C for 10 min and centrifuged at 13,500g during 15 min. Supernatants were diluted in loading buffer and processed immediately or stored at −80 °C.

For the measurement of GSH and antioxidant enzyme activities, samples were thawed, rinsed with 0.9% NaCl and homogenized with phosphate EDTA buffer (100 mM potassium phosphate buffer, pH 7.4, containing 1 mM EDTA).

2.8. Western blotting detection

Protein samples (10 μg from cytosolic and mitochondrial cell extracts or 40–60 μg from placental extracts) were evaluated by the standard protocol performance of Western blot, as previously

Table 1
Primers used for real-time qPCR analysis.

Target gene	Description	Forward primer 5′ → 3′	Reverse primer 5′ → 3′	Amplicon length (bp)
Sdha	Succinate dehydrogenase complex, subunit A, flavoprotein (Fp)	GAGTGCCGTGGTGTCATTG	AAGTAGGTTCGCCCGTAGC	104
Hprt1	Hypoxanthine guanine phosphoribosyl transferase	GGGCTTACCTCACTGCTTTC	TAATCACGACGCTGGGACTG	122
Syp	Synaptophysin	TCAGTGAAGCCCACGAAGAC	GGTTGAGGGGTGGAGACCTA	97
Rpl13a	60 S ribosomal protein L13a	CTCAAGGTTGTTCGGCTGAAG	TTCCGTTTCTCCTCCAGAGTG	113
Actb	Beta actin	TCCAGCAGATGTGGATCAG	AAACGCAGCTCAGTAACAGTCC	98
Dstn	Destrin (ADF—actin-depolymerizing factor)	ATGGATGACACGGGACTG	GCCAGCGTTGCTACTAAG	112
Gsn	Gelsolin (actin regulation)	TACCTCTCCAGCCACATTG	GCCAGTTCCATCATCATCC	111
Cfl1	Cofilin (actin regulation)	TCTGTCTCCCTTTCGTTTCC	GCCTTCTTGCGTTTCTTCAC	130
Cttn	Cortactin (cortical actin binding protein)	TGCTGGTGCCGGTAATCATTG	GCAGAGGCTTTCCACATCTTTC	121
Limk	LIM-kinase (cofilin phosphorylation)	GCGAGGTGATGGTGATGAAGG	GAGCACTCCGATGAACTTG	125
Gpx1	Glutathione peroxidase 1	CCACGTGATCTCAGCACCATCC	CCGAGCAGCACACATACTGGAG	107

described (Farina et al., 2009; Vendrell et al., 2010; Briz et al., 2011) using the specific antibodies, including: Cofilin 1 (for total cofilin), P-Cofilin 1(Ser-3) (for phosphorylated cofilin in serine 3), β-actin and ATP synthase β (ATPβ) diluted 1/1000–1/2000 in TBS-Tween (50 mM Tris/HCl, pH 7.5, 150 mM NaCl, 0.05% Tween-20). Protein content was quantified by the Bradford method. Actin was used as a loading control for placental homogenates whereas protein loading was monitored using the Bradford method for fractional cell extracts due to the fact that actin was translocated from cytosol to mitochondria in MeHg-exposed cells (see the Results section). Other cytosolic protein markers like tubulin or GAPDH were not used as loading control since they were altered by exposure to MeHg (Stern et al., 2014; Popova and Jacobsson, 2014; Wolf and Baynes, 2007). Band intensity was quantified by using the Quantity one 1D-analysis software (Bio-Rad Laboratories, Madrid, Spain).

2.9. RNA purification, reverse transcription and RT-qPCR

Cell samples were harvested by centrifugation and total RNA extractions were performed using the Roche RNeasy kit according to the manufacturer's instructions (Mannheim, Germany). RNA concentrations were calculated by measuring absorbance at 260 nm using a NanoDrop 1000 Spectrophotometer (Thermo Fisher Scientific SL, Alcobendas, Spain). cDNA was synthesized using TaqMan Reverse Transcription Reagents (Applied Biosystems) as recommended. Absence of chromosomal DNA contamination was confirmed by real-time PCR. Reverse transcription and real-time qPCR were performed as previously described (Olguín et al., 2015). Primers were designed (Table 1) to be about 18–22 bases long, to contain over 50% G/C and to have a melting temperature (Tm) above 60 °C. The length of the PCR products ranged from 97 to 125 bp. Clone Manager Professional Suite software and ABI Primer Express program (Applied Biosystems) were used to select primer sequences, and analyze secondary structures and dimer formation.

Real-time PCR was performed in 25 μl final volume containing 10 ng of cDNA, 250 nM of each primer, RNAse free-water and 12.5 μl of SYBR Green Master Mix (Applied Biosystems). Amplifications were carried out using CFX96 Real-Time PCR Detection System (Bio-Rad) with an initial step at 95 °C for 10 min followed by 40 cycles of 95 °C for 15 s, 60 °C for 1 min and 72 °C for 30 s. An additional step starting between 90 and 60 °C was performed to establish a melting curve, and was used to verify the specificity of the real-time PCR reaction for each primer pair.

The efficiencies of amplifications were calculated using the formula $E = [10^{(1/-s)} - 1] \times 100$, where s is the slope of standard curve with several dilutions of cDNA. In this study, the threshold value was automatically determined by the instrument. Results

were analyzed using the comparative critical threshold ($\Delta \Delta C_T$) method in which the amount of target RNA was adjusted to a reference (internal target RNA) as previously described (Livak and Schmittgen, 2001). In order to determine the expression stability for each of the candidate reference genes, 2 different statistical algorithms were applied: NormFinder (Andersen et al., 2004) and BestKeeper (Pfaffl et al., 2004).

2.10. Glutathione (GSH) levels and GSH related enzymes

GSH and the activity of their related enzymes glutathione reductase (GR) and glutathione peroxidase (Gpx) were determined as previously reported (Farina et al., 2009)

2.11. Statistical analysis

Variables are reported as mean values ± SEM calculated for at least three independent experiments. One-way ANOVA and two-way ANOVA followed by post-hoc comparison Dunnett and Bonferroni's tests, respectively, were used for comparing all groups studied. Student's *t*-test was used when comparing only two independent experimental conditions. Data were analyzed using GraphPad Prism v.4 for Windows.

3. Results

3.1. Methylmercury induced cytotoxicity and protein oxidation

We have previously reported that the loss of cell viability induced by MeHg in cultured CGC is time- and concentration-dependent with mean LC50 values ranging from 508 to 243 nM after exposure for 6–16 DIV, respectively (Vendrell et al., 2010). The effect of MeHg on cell viability in both CCN and CGC were determined by the addition of different MeHg concentrations (0–600 nM) from DIV 1 to DIV 9 (Fig. 1). Cell viability determined at 9 DIV was significantly reduced at 300 nM and 600 nM of MeHg in comparison with the vehicle treatment in both CCN (81.8 ± 3.0% and 70.4 ± 5.2%, respectively) and CGC (57.3 ± 19.7% and 30.7 ± 5.6%, respectively) (Fig. 1). Furthermore, toxicity induced by exposure to 600 nM from DIV1 to DIV 9 was significantly higher in CGC than in CCN (p = 0.03). Cytotoxicity induced by 300 nM MeHg was prevented by 10 μM PB (Fig. 1, top insets). When cells were exposed to 300 nM MeHg for a shorter period (5 DIV), cell viability was 88.7 ± 1.8% and 95.6 ± 7.4% of CCN and CGC control cells, respectively (n = 2–3).

We have previously demonstrated that MeHg induces lipid peroxidation in CGC (Vendrell et al., 2007; Farina et al., 2009) as a result of the production of ROS (Gassó et al., 2001). We wonder
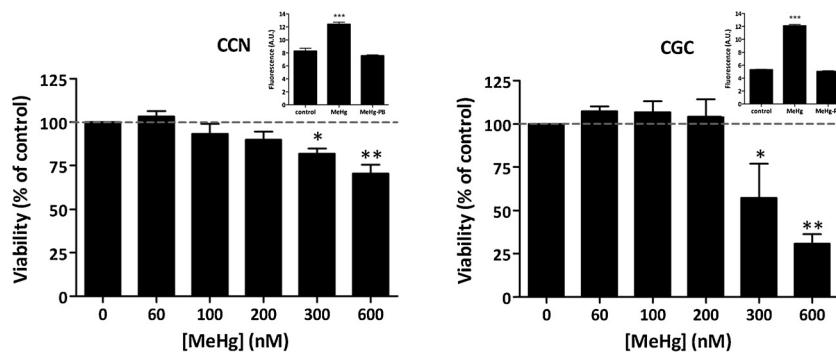

Fig. 1. Concentration-dependent MeHg-induced cytotoxicity in primary cultures of cortical neurons (CCN, left) and cerebellar granule cells (CGC, right). Cells were exposed to MeHg from day in vitro (DIV) 1 to DIV 9. Cell viability was evaluated at 9 DIV by the reduction of MTT. Results are expressed as percent of survival cells compared to control values. Data are expressed as mean ± SEM (N = 3 independent experiments). *p < 0.05 and **p < 0.01 when compared to respective controls by one-way ANOVA and Dunnett's Multiple Comparison Test. Top insets: Protection by 10 μM PB against 300 nM MeHg exposure, as determined by the propidium iodide uptake assay.

whether MeHg-induced ROS led to generalized protein oxidation. Both CCN and CGC showed an increase of protein carbonyls in the presence of MeHg in a concentration-dependent manner. Exposure to 200 nM from DIV 1 to DIV 9, which did not cause cell death (Fig. 1), resulted in a significant increase of carbonylation (Fig. 2A). Furthermore, we have exposed primary cultures of CCN and of CGC to 300 nM MeHg during 5 DIV in order to detect proteins oxidation in advance to the induction of cell death. Fig. 2B shows that exposure to 300 nM MeHg for a shorter period (DIV 1 to DIV 6) induced a significant increase of protein carbonylation that was prevented by the antioxidant PB.

3.2. Cell-type dependent cofilin and actin translocation to mitochondria by MeHg is prevented by probucol

Primary cultures of CCN and CGC were exposed to 300 nM of MeHg in the presence or the absence of 10 μM PB for 5 DIV in order to detect cofilin localization in cytosolic and mitochondrial extracts. Western blot was used to detect the presence of this protein as well as the presence and localization of Ser3 phosphorylated cofilin (P-Cofilin). It is important to notice that β-actin (actin) and ATP synthase β (ATPSβ) levels were initially taken as sample loading control for cytosol and mitochondrial extracts, respectively. However, it soon turned out that actin also translocates to the mitochondria after MeHg exposure (Figs. 3 and 4 top). Therefore, load control was taken on the basis of protein content and 10 μg of cytosolic or mitochondrial extracts were always submitted to electrophoresis and analyzed by Western blot. In both CCN and CGC control cells we found an exclusive cytosolic localization of both cofilin and P-cofilin, together with cytosolic localization of actin and mitochondrial localization of ATPSβ, using this latter as control of mitochondrial isolation (western blot bands in Figs. 3 and 4, top).

After treatment of CCN (Fig. 3), cofilin maintained a cytosolic localization in all conditions (control, 300 nM MeHg and MeHg plus PB) with no statistical difference between groups (Fig. 3A). On the contrary, cytosolic P-cofilin levels in CCN were reduced in the presence of MeHg (Fig. 3C). In addition the P-cofilin/cofilin ratio was also reduced with respect to unexposed cells ($p < 0.05$). However, P-cofilin maintained control levels when PB was present

($p < 0.05$) compared to cells treated only with MeHg (Fig. 3B and C). Moreover, we observed a clear translocation of actin from cytosol to mitochondria after MeHg exposure (Fig. 3B). In this way, actin levels were significantly reduced in cytosolic extracts from CCN treated with 300 nM MeHg (Fig. 3B, left) whereas an increasing level of actin was observed in mitochondrial extracts in comparison to unexposed cells ($p < 0.01$) (Fig. 3B, right). Co-treatment of MeHg with PB maintained actin levels similar to control values in both cell extracts ($p < 0.05$) (Fig. 3B).

In the case of CGC, a significant decrease of cofilin ($p < 0.01$) and actin ($p < 0.05$) levels in the cytosol was observed after 300 nM MeHg treatment (Figs. 4A–B, left). On the contrary, a significant increase of cofilin and actin levels was observed in mitochondrial extracts (Fig. 4A–B, right) in comparison to unexposed cells ($p < 0.01$). Likewise, P-cofilin levels localized in the cytosol were significantly reduced ($p < 0.01$) when CGC were exposed to 300 nM MeHg in comparison to control cells (Fig. 4C). P-cofilin was not found in the mitochondrial extracts of MeHg-exposed cells. These results suggest that both cofilin and actin were translocated from the cytosol to the mitochondria in CGC exposed to MeHg. They also show that the non-phosphorylated form of cofilin was the translocated protein.

Furthermore, co-treatment of MeHg with PB prevented both cofilin and actin translocation to mitochondria (Fig. 4A–B). In this way, the MeHg-induced increase in cofilin and actin levels in the mitochondria was prevented by PB ($p < 0.05$) (Fig. 4A–B; right). A similar effect was observed in the cytosol where the reduced levels of cofilin and actin in the presence of MeHg were maintained at control levels in presence of PB ($p < 0.05$) (Fig. 4A–B, left). Likewise, the reduced P-cofilin levels in the cytosolic fraction induced by MeHg were also maintained at control levels by PB ($p < 0.05$) (Fig. 4C).

3.3. Cofilin and actin translocation to mitochondria is dependent on MeHg concentration in CGC

Since cofilin was translocated to mitochondria in CGC but not in CCN after the exposure to 300 nM MeHg, we decided to evaluate if this translocation is dependent on MeHg concentration. In addition, we also evaluated actin translocation in these conditions. After 5 DIV
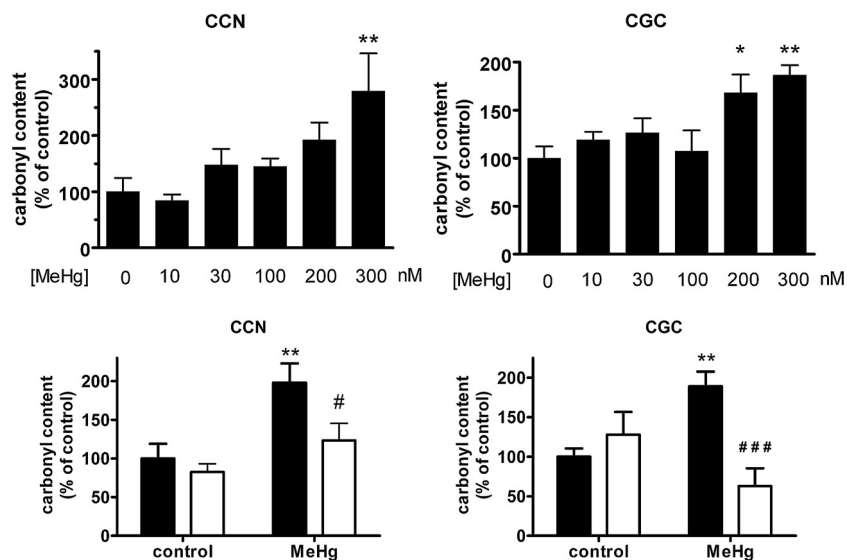

Fig. 2. Carbonyl contents in primary cultures of cerebellar granule cells (CGC) and cortical neurons (CCN) exposed to MeHg. Top) Concentration-response effect in cells exposed to MeHg from DIV 1 to DIV 9. *p < 0.05 and **p < 0.01 compared to control after one-way ANOVA. Bottom) Cells were exposed for 5 DIV to 300 nM MeHg without (black bars) and with (white bars) 10 μM of probucol. **p < 0.01 compared to control in the absence of probucol; #p < 0.05, ###p < 0.001 compared to 300 nM of MeHg by two-way ANOVA. Results are expressed as % of control (mean ± SEM from N = 3–4 independent experiments).
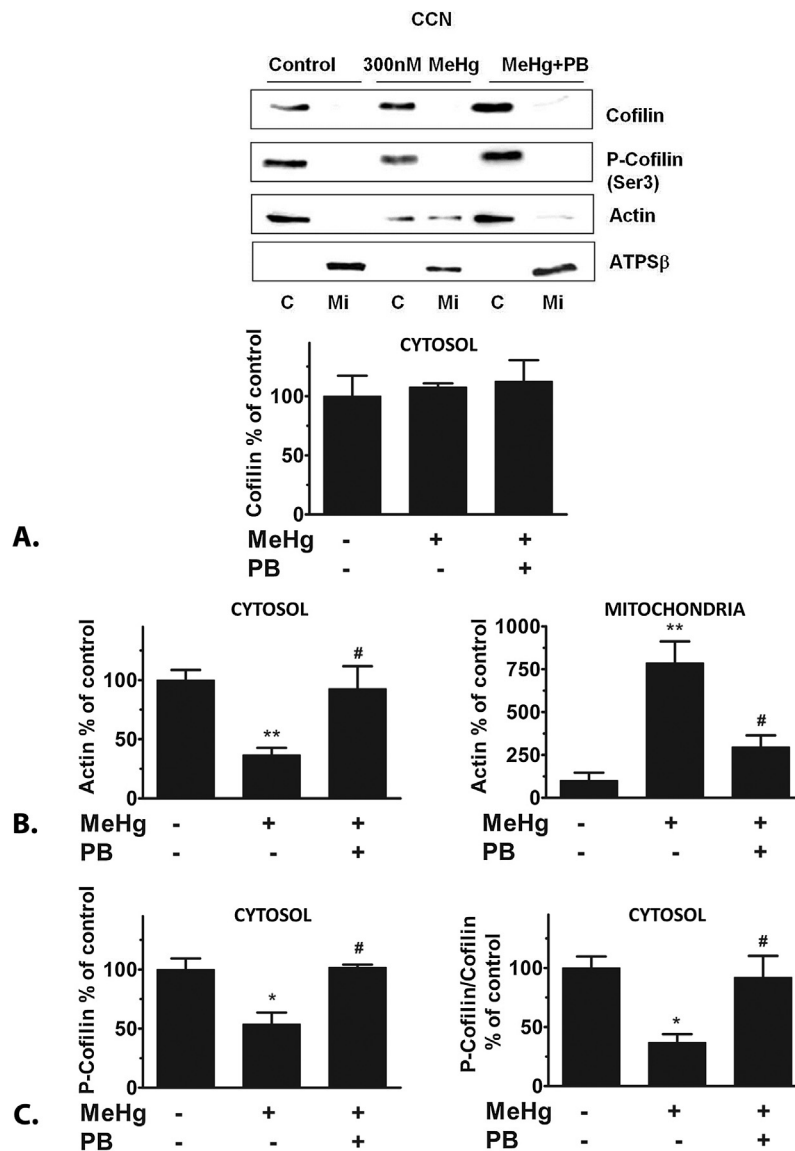
Fig. 3. Total cofilin (Cofilin), phosphorylated Cofilin (P-Cofilin), β-actin (Actin) and ATP synthase β (ATPSβ) proteins were detected by western blotting using 10 μg of protein of cytosolic (C) and mitochondrial (Mi) extracts from primary cultures of CCN exposed to 300 nM MeHg with and without 10 μM of probucol (PB) for 5 DIV. ATPSβ was used as control of mitochondrial isolation. Bar chart showing semi-quantitative optical density (arbitrary units of blot bands as % of control) of cytosolic levels of Cofilin (A), Actin levels in cytosolic (left) and mitochondrial (right) enriched fractions (B), and changes in the cytosolic levels of P-Cofilin and P-Cofilin/Cofilin ratio (C). Data are represented as mean ± SEM (N = 3-4 independent experiments). $^*p < 0.05$, $^{**}p < 0.01$ compared to control; #p < 0.05 compared to 300 nM of MeHg.

exposure to 0–300 nM MeHg a concentration-dependent translocation to mitochondria was observed for both cofilin and actin (Fig. 5). In this way, cofilin and actin levels were reduced in cytosolic extracts as the concentration of MeHg increased (Fig. 5A–B, left). Simultaneously, cofilin and actin levels were significantly increased in mitochondrial extracts with increasing concentrations of MeHg and being statistically significant at a concentration of MeHg as low as 30 nM ($p < 0.05$ and $p < 0.01$, respectively) (Fig. 5A–B, right, respectively). A concentration-dependent decrease in the cytosolic levels of P-cofilin was also observed in CGC treated with MeHg in comparison to control cells (Fig. 5C).

3.4. Independent translocation of cofilin and actin do not affect cell survival in CCN and CGC

Cofilin translocation has been reported to be an early step in apoptosis induction in response to oxidative stress (Chua et al., 2003; Zdanov et al., 2010,). Since CCN and CGC presented a

different translocation pattern of actin and cofilin it was worth to study if this difference could be affecting cell viability. Some authors have pointed out that mitochondrial targeting of cofilin is an essential step for engaging apoptosis through a mechanism where dephosphorylated cofilin binds to unpolymerized globular actin (G-actin), translocates to mitochondria and eventually elicits apoptosis (Chua et al., 2003; Li et al., 2013). On the other hand, actin translocates independently of cofilin to mitochondria during staurosporine-induced apoptosis in cultured fibroblasts (Rehklau et al., 2012). We tested whether JAS, a membrane-permeable peptide that binds to and stabilizes actin microfilaments (F-actin) decreasing the rate of dissociation of actin oligomers and thus depleting G-actin levels (Bubb et al., 1994), could differentially affect MeHg-induced cell death in CGC and CCN. The loss of cell viability induced by 600 nM MeHg was determined in the absence and the presence of 100 nM JAS (Fig. 6). Our results show that pretreatment of CGC or CCN with JAS did not preclude MeHg-induced cell death in both cell types (Fig. 6).
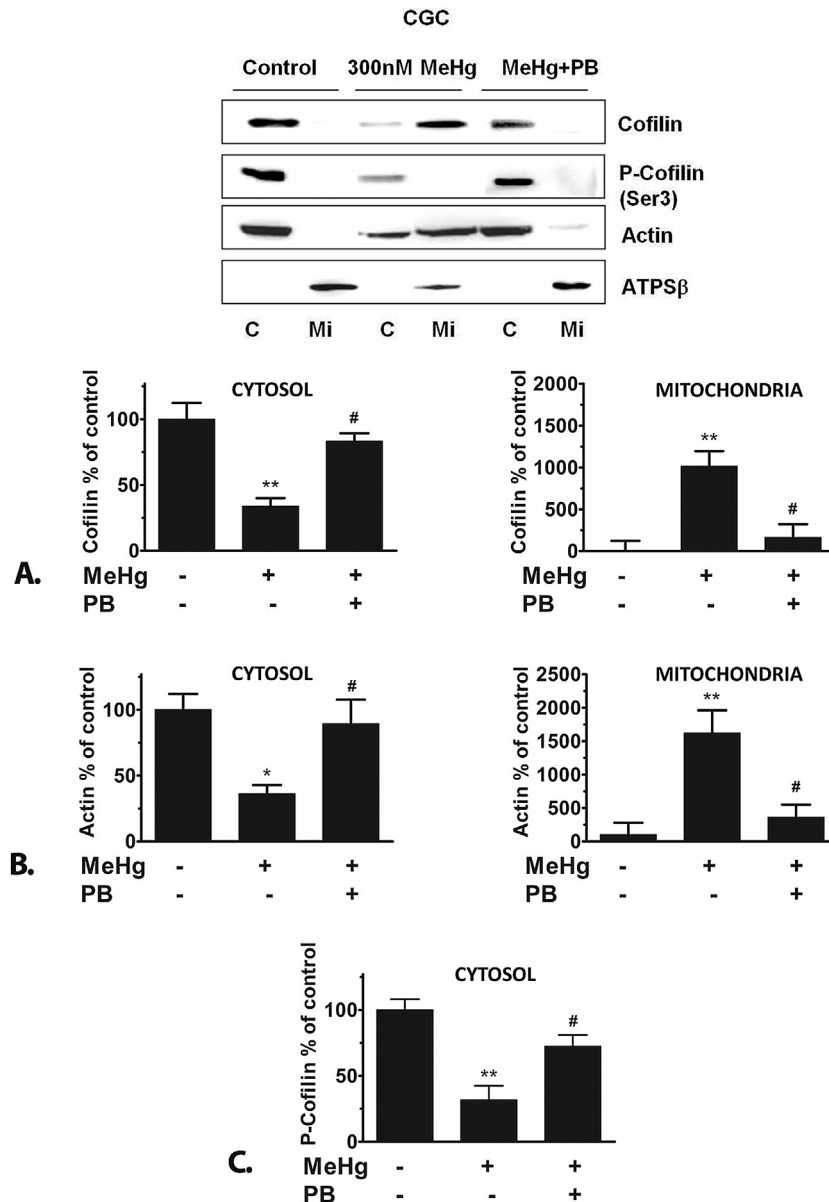
Fig. 4. Total cofilin (Cofilin), phosphorylated Cofilin (P-Cofilin), β-actin (Actin) and ATP synthase β (ATPSβ) proteins were detected by western blotting using 10 μg of protein of cytosolic (C) and mitochondrial (Mi) extracts from primary cultures of CGC exposed to 300 nM MeHg with and without 10 μM of probucol (PB) for 5 DIV. ATPSβ was used as control of mitochondrial isolation. Bar chart showing semi-quantitative optical density (arbitrary units of blot bands as % of control) of Cofilin (A) and Actin (B) levels in cytosolic (left) and mitochondrial (right) enriched fractions, as well as changes in the cytosolic levels of P-Cofilin (C). Data are represented as mean ± SEM (N = 3–4 independent experiments). *p < 0.05, **p < 0.01 compared to control; #p < 0.05 compared to 300 nM of MeHg.

3.5. Transcriptional response of genes related to actin and cofilin dynamics in CCN and CGC

In order to determine if the different translocation behavior of actin/cofilin is linked to cell type and/or genetic regulation, several genes related to the expression of actin/cofilin dynamics and the gene coding for the protein glutathione peroxidase, were chosen for evaluation (Table 1). Gene expression was determined under milder MeHg exposure conditions than those eliciting altered actin/cofilin behavior to evaluate early transcriptional changes. However, we had to discard many of these genes due to poor amplification efficiencies (*Hprt*, *Sdha*, *Gsn* and *Cfl1*). The analysis of expression stability revealed that combination of both *Dstn* and *Actb* was the most suitable for data normalization according to BestKeeper and NormFinder. Therefore, we used the geometric average of these genes for normalization. Data are expressed as means of linearized values from data normalized using the geometrical mean between *Dstn* and *Actb* raw data. Therefore, data are presented as the fold change or relative expression level related to the control condition treated with vehicle. Fig. 7 shows the relative expression levels of *Cttn* (encoding for the cortactin protein, from "cortical actin binding protein"), *Limk* (encoding for LIM kinase which phosphorylates cofilin at Ser3) and *Gpx1* (encoding for the enzyme glutathione peroxidase 1) genes in CGC cells after exposure to MeHg. *Cttn* gene which encodes for the cortactin protein and *Limk* gene which encodes for the LIM-kinase 1 protein showed an increased transcriptional response in presence of MeHg that was significantly reduced by 10 μM PB (Fig. 7A and B). Finally, *Gpx1* was down-regulated in presence of MeHg and of MeHg + PB (Fig. 7C). On the other hand, CCN cells presented no significant change in gene expression among conditions or among genes.
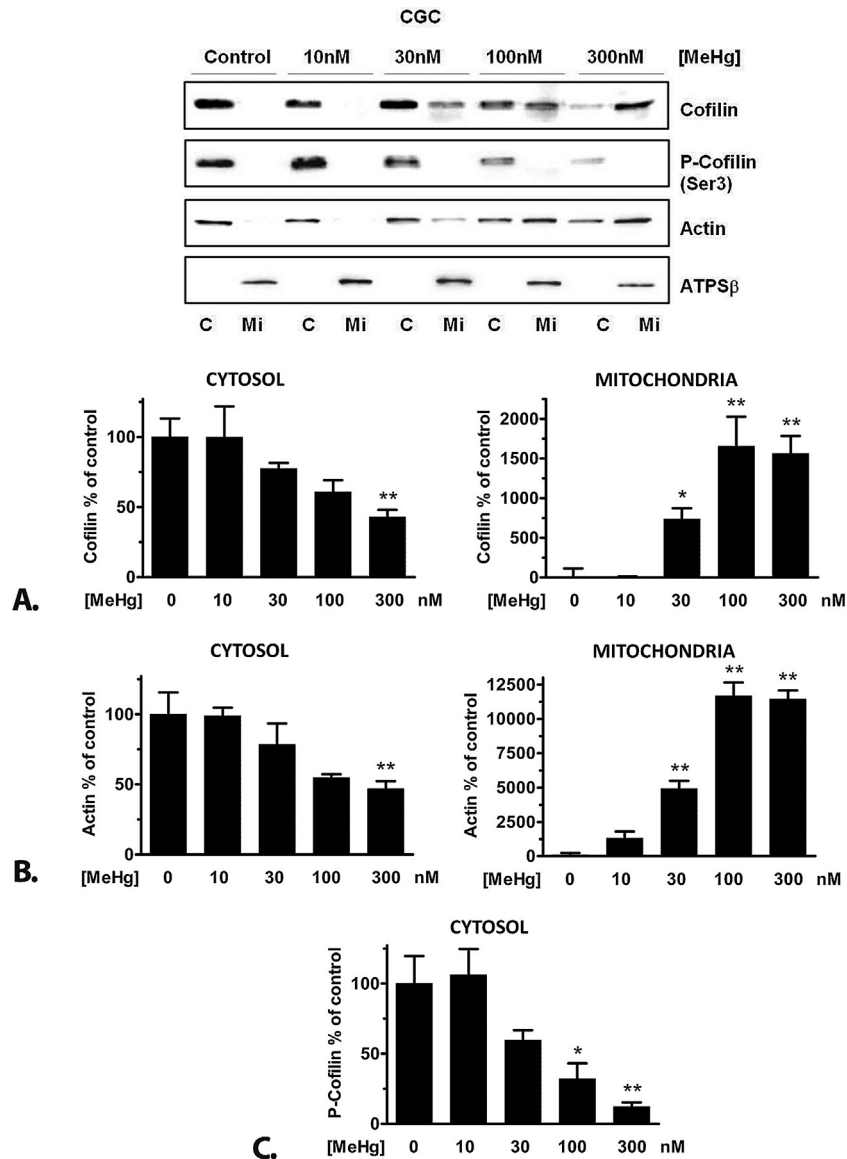
Fig. 5. Concentration-dependent MeHg-induced changes in levels of total cofilin (Cofilin), phosphorylated Cofilin (P-Cofilin), β−actin (Actin) and ATP synthase β (ATPSβ) proteins, using 10 μg of protein of cytosolic (C) and mitochondrial (Mi) extracts from primary cultures of CGC exposed to different concentration of MeHg (0–300 nM) for 5 DIV. ATPSβ was used as control of mitochondrial isolation. Bar chart showing semi-quantitative optical density (arbitrary units of blot bands as % of control) of Cofilin (A) and Actin (B) levels in cytosolic (left) and mitochondrial (right) enriched fractions, as well as changes in the cytosolic levels of P-Cofilin (C). Data are represented as mean ± SEM (N = 3–4 independent experiments). $^*p < 0.05$, $^{**}p < 0.01$ compared to control.
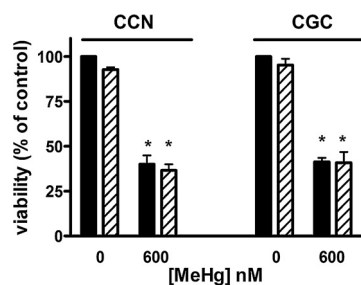

Fig. 6. Effect of jasplakinolide (JAS) on MeHg-induced cell death in primary cultures of cortical neurons (CCN) and of cerebellar granule cells. Cells were seeded at 8×10^5 cells/mL and treated with vehicle (DMSO) or 100 nM JAS for 15 min at DIV 1, rinsed, and thereafter exposed to 600 nM MeHg for 4 DIV. Data are expressed as mean ± SEM (N = 3 independent experiments). $^*p < 0.001$ with respect to control.

3.6. P-cofilin expression and antioxidant enzymes activity are decreased in human placentas in relation to MeHg prenatal exposure

Prenatal exposure to drugs/pollutants generally occurs via their transfer through placenta. In fact, although the placenta transports nutrients and oxygen and acts as mother-child barrier, it also transports many foreign compounds. Particularly, MeHg is effectively transported by the placenta attaining higher concentrations in the cord blood (fetal side) than in the maternal blood (Björnberg et al., 2005; Sakamoto et al., 2013). In an attempt to find biological markers of fetal MeHg exposure and affectation, we examined P-cofilin expression in a subset of placental homogenates (both from the maternal and fetal side) corresponding to individuals who have had their levels of mercury exposure characterized (Ramon et al., 2011). Placental samples were analyzed by Western blot to determine the levels of P-cofilin
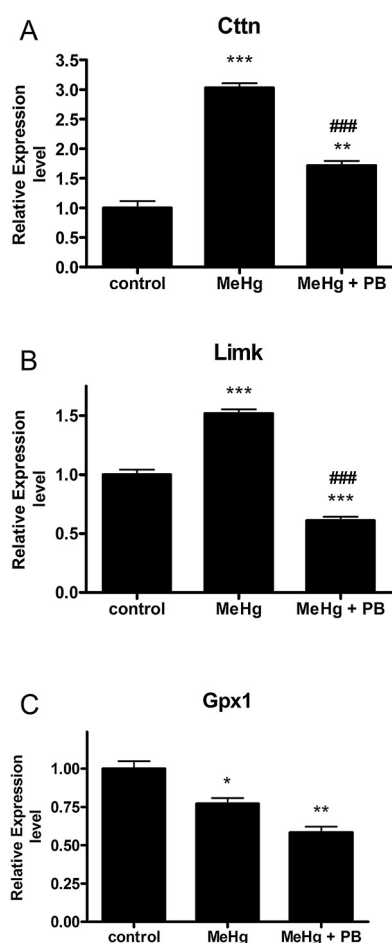
Fig. 7. Relative expression levels of three genes related to actin/cofilin dynamics in primary cultures of cerebellar granule cells (CGC) exposed to 100 nM MeHg with and without 10 μM of probucol (PB) for 20 h. Data was normalized using the average of Actb and Dstn reference genes. The relative expression values of *Cttn* (A), *Limk* (B) and *Gpx1* (C) are depicted as mean ± SEM (N = 3 independent experiments). Bars represent the fold change related to control group (20 h) which was set to 1 in order to normalize the results. *p < 0.05, **p < 0.01 and ***p < 0.001 in comparison to the control condition and ###p < 0.001 in comparison to MeHg treatment in the absence of PB by one-way ANOVA and Bonferroni's Multiple Comparison Test.

Fig. 8. Phosphorylated Cofilin (P-Cofilin) and β-actin (Actin) proteins were detected in human placental samples by western blotting. Top: Representative Western blot bands corresponding to the fetal and maternal sides of individual samples (figures indicate the anonymous code of the sample). Bottom: Bar chart showing semi-quantitative optical density of P-cofilin in the maternal and fetal side of the placentas normalized to their corresponding actin levels. Diagonal bars correspond to samples characterized by low Hg exposure (<7 μg/L Hg in their associated cord blood) and vertical bars correspond to samples characterized by high Hg exposure (20–40 μg/L Hg in their associated cord blood). Data are represented as mean ± SEM of 12 and 9 samples from the maternal and fetal side, respectively. *p < 0.05, Student's *t*-test.

4. Discussion

4.1. Protein oxidation precedes cell death in MeHg-exposed primary cultures of cortical neurons and of cerebellar granule cells

The results presented herein show that prolonged exposure (≥5 DIV) to MeHg in both CGC and CCN primary cultures was significantly associated with increased cell death, which was preceded by increased levels of protein carbonyl groups. These effects were prevented by co-treatment with the antioxidant PB. We have previously described that the molecular events involved in MeHg-induced neurotoxicity in CGC were associated with an increased oxidative stress, by means of a decrease in antioxidant Gpx1 activity and an increase in lipid peroxidation, which were all prevented by the antioxidant effect of probucol (Vendrell et al., 2007; Farina et al., 2009). In accordance with the results of the present study, the treatment and supplement with antioxidants has been shown to prevent, or at least to diminish, the toxicological effect of MeHg *in vitro* (Dare et al., 2000; Fonfría et al., 2005; Farina et al., 2009; Zhang et al., 2009; Falluel-Morel et al., 2012).

4.2. MeHg-induced cofilin dephosphorylation, actin translocation to mitochondria and cell type-dependent cofilin translocation to mitochondria is prevented by the antioxidant probucol

In previous studies, we have reported that MeHg induces dephosphorylation of the actin binding protein cofilin in CGC (Vendrell et al., 2010). In this work, we have extended this study to cortical neurons corroborating that MeHg induces cofilin

normalized to actin levels. It should be noticed that total actin levels are not modified by MeHg exposure (Miura et al., 1998; Vendrell et al., 2007, 2010) thus allowing the use of this protein as loading control in tissue homogenates. The placental samples were related to individuals with low and high exposure to MeHg, as determined by the Hg levels in their corresponding cord blood (<7 μg/L and 20–40 μg/L for low and high levels of Hg, respectively). Fig. 8 shows that P-cofilin levels were significantly reduced in the fetal side of the subset of placentas corresponding to the highest fetal exposed group with respect to the lowest exposed group (p = 0.02).

Exposure to MeHg induces a reduction of endogenous antioxidant defenses in both cellular and animal models (Stringari et al., 2008; Farina et al., 2009). We have determined glutathione concentration (measured as non-protein sulfhydryl—NPSH), and glutathione reductase and glutathione peroxidase activities in the above placental samples. Fig. 9 shows that MeHg exposure (high *vs* low Hg levels in cord blood) did not produce significant changes in the studied parameters, however a decreasing trend was found for GR and Gpx activities in the fetal side and an increasing trend was found for GSH in the maternal side.
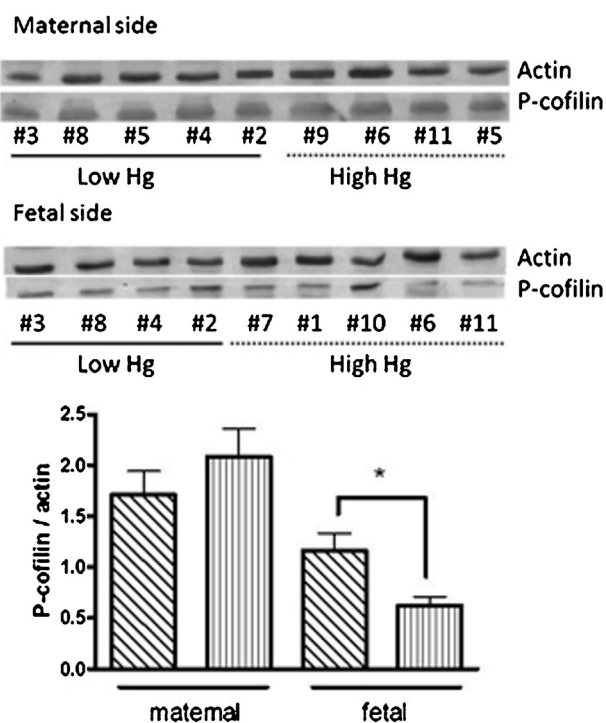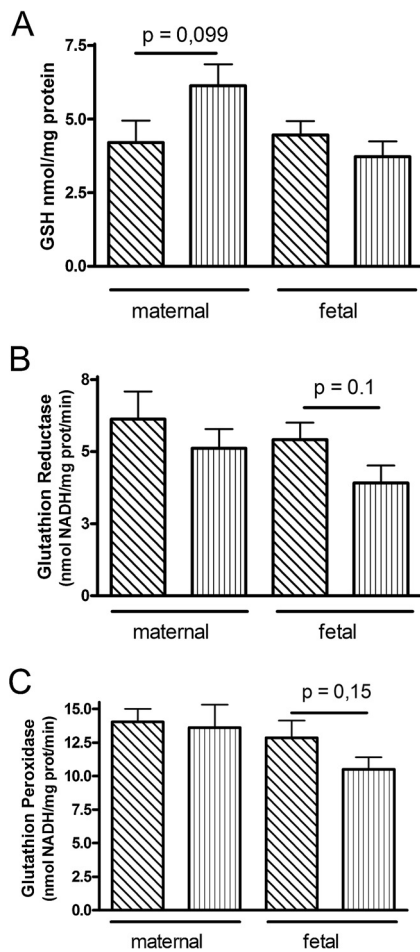
Fig. 9. Glutathione levels (A), glutathione reductase activity (B) and glutathione peroxidase activity (C) in placental samples. Diagonal bars correspond to samples characterized by low Hg exposure ($<7\,\mu g/L$ Hg in their associated cord blood; n = 4–5 and 5 for the maternal and fetal side, respectively) and vertical bars correspond to samples characterized by high Hg exposure ($20–40\,\mu g/L$ Hg in their associated cord blood; n = 7 and 6 for the maternal and fetal side, respectively). Data are represented as mean ± SEM.

dephosphorylation in both cell types, CCN and CGC. An important finding from the present study was that, in addition to suffering dephosphorylation in response to MeHg, cofilin translocates from the cytosol to the mitochondria, but this mechanism was dependent on the cell type since mitochondrial cofilin translocation was only detected in MeHg-exposed CGC, but not in CCN. In fact, mitochondrial cofilin translocation in CGC was observed from MeHg concentrations as low as 30 nM. It is important to note that cofilin is also a key target of oxidation (Gourlay and Ayscough, 2005) and, in this way, not only dephosphorylation of cofilin but also its oxidation in response to MeHg-induced oxidative stress may be necessary for it to translocate to mitochondria (Chua et al., 2003). This hypothesis was corroborated by treatment with the antioxidant PB, which reduced oxidized proteins and maintained cofilin phosphorylation and cell viability. MeHg-induced cofilin translocation to mitochondria in CGC is in agreement with previous reports describing that mitochondrial cofilin translocation mediates apoptotic cell death in response to oxidative stress (Chua et al., 2003; Zdanov et al., 2010), even as an early step in apoptosis induction. On the other hand, it has also been suggested that cofilin activity is not generally required for induction or progression of apoptosis in mammalian cells (Rehklau et al., 2012). Our results suggest that this may depend on cell type since cofilin translocation to

mitochondria was observed in CGC but not in CCN. In this scenario, one may posit that the different behavior of cofilin regarding its translocation into mitochondria in CGC and CCN could be accounted for by different mitochondria downstream apoptotic-related cascade involving caspases in these cells after MeHg exposure. It is well known that MeHg disrupts a wide variety of cellular processes so it is difficult to pinpoint individual or specific factors that may contribute to the differential cellular neurotoxicity effects of MeHg. Thus, cofilin might be part of a molecular pathway that contributes to a different sensitivity and/or response to MeHg between GCC and CCN. Furthermore, *Limk* and *Cttn* gene expression (related to cofilin phosphorylation and to actin/cofilin dynamics, respectively) was significantly altered in CGC but not in CCN. The different cell-type sensitivity to MeHg is also a hallmark of the pathological findings after MeHg poisoning in humans where a specific loss of defined neuronal types (like granule cells in the cerebellum and neurons in the auditory cortices and in the anterior area of the calcarine fissure of the occipital lobe) is found whereas other brain areas and neuronal cell types are much less damaged or even free of lesions (Sanfeliu et al., 2003).

Moreover, we have observed actin translocation to mitochondria, in this case in both CGC and CCN primary cultures exposed to low doses of MeHg (30–300 nM), which was prevented by PB co-exposure. Accumulating evidence indicates the potential role of cytoskeletal actin in apoptosis (Utsumi et al., 2003; Li et al., 2004; Tang et al., 2006). In this sense, it was observed that actin translocates independent of cofilin or ADF to mitochondria during apoptosis (Rehklau et al., 2012). Actin participates in both apoptotic and necrotic pathways. It seems that actin itself can reach the mitochondria either directly or indirectly through intermediated proteins to promote apoptosis. The latest can be produced by means of cofilin, which can act as mitochondrial shuttle for actin, or after being cleaved by a caspase-3-like activity to generate a 15 kDa fragment, which after being modified by N-myristoylation it targets the mitochondria and stimulates apoptosis (Utsumi et al., 2003; Wang et al., 2008). In most cases, the mechanism of cell death has been directly attributed to the pro-apoptotic properties of actin (Tang et al., 2006; Wang et al., 2008), which is in agreement with the findings of this work, in which we observed mitochondrial translocation of actin and cell death in both CCN and CGC. However, cytoskeletal proteins such as cofilin can serve as mitochondrial shuttles for actin (Wang et al., 2008). It is important to note that CGC showed mitochondrial translocation of both, actin and cofilin, at the same concentrations of MeHg. However, these translocations probably occur independently, since the domain of cofilin involved in actin binding was suggested to be indispensable for its pro-apoptotic functions but not for its mitochondrial localization (Chua et al., 2003). In fact, oxidation of all four cysteine residues in cofilin is required for it to undergo mitochondrial translocation and gain its pro-apoptotic function in response to oxidants. But after this oxidation cofilin undergoes a conformational change that leads to lose its ability to bind to actin (Gourlay and Ayscough, 2005; Klamt et al., 2009), supporting the idea that cofilin goes to mitochondria without actin binding. In a recent study, Rehklau and col. (2012) have demonstrated that impaired mitochondrial association of cofilin and ADF in response to treatment with either JAS or phalloidin, two peptides that block the interaction of ADF/cofilin with actin, significantly reduced the mitochondrial translocation of cofilin and ADF and that this reduced mitochondrial association is the result of impaired actin interaction. Aiming to demonstrate if translocation of actin but not cofilin was responsible for the differences in CCN and CGC vulnerability against MeHg we also treated these cells with JAS. Our results did not show any significant difference regarding cell viability between controls

and JAS treated cells. Therefore, we hypothesize that actin translocation may be the key event in the process for cell death signaling in most cells whereas cofilin translocation may be involved in some, but not all, type of cells. Nonetheless, it should be considered that cytosolic P-cofilin was indeed reduced in both CCN and CGC.

4.3. MeHg-induced changes in genes related to cofilin and actin dynamics is cell type-dependent

In order to investigate about the cell-type differences we decided to study the transcriptional response of some genes related to actin/cofilin dynamics in CCN and CGC. We were able to determine that gene expression is significantly different between CCN and CGC. Whereas there is no observable change of expression response among conditions in CCN for any of the tested genes, CGC did display some transcriptional differences among conditions and among the different genes. *Cttn* gene which codes for the protein cortactin (from "cortical actin binding protein"), was overexpressed in CGC in all conditions. It was previously found that mitochondrial division and mitochondrial assembly of F-actin is controlled by the actin regulatory proteins cortactin, cofilin, and Arp2/3 complexes (Li et al., 2015a). Our results indicate that in addition to mitochondrial translocation of cofilin, cortactin could be also involved in a different response between CCN and CGC if its involvement is transcriptionally dependent. However, a more in depth evaluation of *Cttn* transcriptional response is needed in order to test this hypothesis. In addition, we analyzed the relative expression level of *Limk* gene which codes for the LIM kinase 1 protein. This protein phosphorylates and thereby inhibits the effects of cofilin on the actin cytoskeleton by reducing the pool of active cofilin (Arber et al., 1998). Our results demonstrated that *Limk* was overexpressed in CGC treated with MeHg but downexpressed when PB was present. However, the interpretation of these results is somewhat unclear since MeHg induced cofilin dephosphorylation. It has been reported that LIMK1 is activated in response to apoptotic stimulus (Mizuno, 2013) and we and others have reported that MeHg induces apoptosis in cerebellar granule cells (Vendrell et al., 2007; Dare et al., 2000; Castoldi et al., 2000). On the other hand, LIMK 1 is not the only pathway that regulates cofilin phosphorylation and the slingshot family protein phosphatases (SSHs) decrease the level of P-cofilin. In fact, in cultured neurons there is a local and temporal regulation of cofilin phosphorylation by LIMK 1 and SSHs (Mizuno, 2013). The mechanistic scenario involving *Limk*- and cofilin-mediated apoptosis seems to be not completely understood and further studies are necessary in this topic.

Additionally, gene expression of Gpx-1 protein was analyzed in order to determine if the overexpression of this protein (Farina et al., 2009) is transcriptionally determined. Our results show that *Gpx1* was down expressed in the presence of MeHg and that coexposure with probucol did not revert this effect. We have previously shown that PB increases GPx-1 activity in CGC cultures inducing an enduring protection against MeHg toxicity without modifying GPx-1 protein levels (Farina et al., 2009). According to the results shown here, we demonstrate that the actual exposure to MeHg in CGC and CCN transcriptionally affected *Cttn*, *Limk* and *Gpx-1* expression in CGC but not in CCN, which may or may not be affecting a differential response between CCN and CGC response to MeHg-induced toxicity. It is also unclear if the transcriptional response may be related to the observed cofilin translocation in CGC. Further studies should be carried out in order to determine this possibility. However, despite discrepancies between studies related to cofilin translocation to mitochondria, actin translocation to mitochondria and cofilin dephosphorylation appear to play a crucial role in regulating the cell response to the neurotoxicity induced by MeHg.

4.4. Human prenatal exposure to MeHg leads to disrupted cofilin phosphorylation/dephosphorylation regulation and to reduced activity of endogenous antioxidant defenses

In addition to the investigation of mechanisms mediating MeHg-induced toxicity in cultured neurons, we also performed parallel studies in placental samples derived from humans exposed to MeHg. Of note, we observed that MeHg exposure caused a significant decrease in the levels of P-cofilin; however, this was observed only in placental samples derived from the fetal, but not maternal side. We also observed a trend (p value near to 0.1) of decreasing GPx and GR activities in MeHg-exposed subjects, but this was also observed only in placental samples derived from the fetal side. The fact that higher concentrations of MeHg are attained in the cord blood (fetal side) than in the maternal blood (Björnberg et al., 2005; Sakamoto et al., 2013) may support the differences found between the maternal and fetal side of the placentas. Mercury levels in the cord blood of the highly exposed subjects studied in this work account for 100–200 nM. Cultured neuronal cells and placental samples exposed to 100–200 nM MeHg have in common a reduced level of P-cofilin. Thus, our results suggest that decreased levels of P-cofilin might represent an important event mediating MeHg-induced toxicity, which is not limited to cultured neurons exposed to MeHg under *in vitro* conditions. In addition, the observed decreased activities of GPx and GR in placental samples derived from MeHg-exposed subjects reinforce the important role of pro-oxidative events in mediating MeHg-induced changes in cofilin homeostasis, corroborating our *in vitro* results derived from experiments with cultured neurons.

5. Conclusions

The results of this study show that exposure to MeHg induced dephosphorylation of cytosolic cofilin and translocation of actin from the cytosol to the mitochondria in both cultured cerebellar granule cells and cortical neurons. Furthermore, non-phosphorylated cofilin was translocated from the cytosol to the mitochondria in cerebellar granule cells but not in cortical neurons, thus providing a new molecular pathway that might account for the higher vulnerability of cerebellar granule neurons against MeHg. All these effects and those showing MeHg-induced reduced cell viability and increased protein carbonylation were prevented by the action of the antioxidant probucol. Therefore, oxidative stress is a primary factor of MeHg-induced neurotoxicity in cultured neurons. In the translational study using human samples we also show that higher levels of prenatal Hg exposure were associated with a reduction of phosphorylated cofilin in the placental fetal side. Also, the decreased activities of endogenous antioxidant enzymes GPx and GR in placental samples derived from MeHg-exposed subjects reinforce the important role of pro-oxidative events in mediating MeHg-induced toxicity. In summary, cofilin dephosphorylation and oxidative stress are hallmarks of MeHg exposure in experimental cellular systems and human samples.

Conflict of interest

The authors have declared no conflict of interest.

Acknowledgements

References

Andersen, C.L., Jensen, J.L., Ørntoft, T.F., 2004. Normalization of real-time quantitative reverse transcription-PCR data: a model-based variance estimation approach to identify genes suited for normalization, applied to bladder and colon cancer data sets. Cancer Res. 64, 5245–5250.

Arber, S., Barbayannis, F.A., Hanser, H., Schneider, C., Stanyon, C.A., Bernard, O., Caroni, P., 1998. Regulation of actin dynamics through phosphorylation of cofilin by LIM-kinase. Nature 393, 805–809.

Björnberg, K.A., Vahter, M., Berglund, B., Niklasson, B., Blennow, M., Sandborgh-Englund, G., 2005. Transport of methylmercury and inorganic mercury to the fetus and breast-fed infant. Environ. Health Perspect. 113, 1381–1385.

Briz, V., Molina-Molina, J.M., Sanchez-Redondo, S., Fernandez, M.F., Grimalt, J.O., Olea, N., Rodriguez-Farre, E., Suñol, C., 2011. Differential estrogenic effects of the persistent organochlorine pesticides dieldrin, endosulfan, and lindane in primary neuronal cultures. Toxicol. Sci. 120, 413–427.

Bubb, M.R., Senderowicz, A.M.J., Sausville, E.A., Duncan, K.L.K., Korn, E.D., 1994. Jasplakinolide, a cytotoxic natural product: induces actin polymerization and competitively inhibits the binding of phalloidin to F-actin. J. Biol. Chem. 269 (21), 14869–14871.

Castoldi, A.F., Barni, S., Turin, I., Gandini, C., Manzo, L., 2000. Early acute necrosis: delayed apoptosis and cytoskeletal breakdown in cultured cerebellar granule neurons exposed to methylmercury. J. Neurosci. Res. 59, 775–787.

Castoldi, A.F., Coccini, T., Ceccatelli, S., Manzo, L., 2001. Neurotoxicity and molecular effects of methylmercury. Brain Res. Bull. 55, 197–203.

Ceccatelli, S., Dare, E., Moors, M., 2010. Methylmercury-induced neurotoxicity and apoptosis. Chem. Biol. Interact. 188, 301–308.

Chua, B.T., Volbracht, C., Tan, K.O., Li, R., Yu, V.C., Li, P., 2003. Mitochondrial translocation of cofilin is an early step in apoptosis induction. Nat. Cell Biol. 5, 1083–1089.

Dare, E., Gotz, M.E., Zhivotovsky, B., Manzo, L., Ceccatelli, S., 2000. Antioxidants J811 and 17beta-estradiol protect cerebellar granule cells from methylmercury-induced apoptotic cell death. J. Neurosci. Res. 62, 557–565.

Dare, E., Gorman, A.M., Ahlbom, E., Gotz, M., Momoi, T., Ceccatelli, S., 2001. Apoptotic morphology does not always require caspase activity in rat cerebellar granule neurons. Neurotox. Res. 3, 501–514.

Do Nascimento, J.L., Oliveira, K.R., Crespo-Lopez, M.E., Macchi, B.M., Maues, L.A., Pinheiro Mda, C., Silveira, L.C., Herculano, A.M., 2008. Methylmercury neurotoxicity & antioxidant defenses. Indian J. Med. Res. 128, 373–382.

Ekino, S., Susa, M., Ninomiya, T., Imamura, K., Kitamura, T., 2007. Minamata disease revisited: an update on the acute and chronic manifestations of methyl mercury poisoning. J. Neurol. Sci. 262, 131–144.

Falluel-Morel, A., Lin, L., Sokolowski, K., McCandlish, E., Buckley, B., DiCicco-Bloom, E., 2012. N-acetyl cysteine (NAC) treatment reduces mercury-induced neurotoxicity in the developing rat hippocampus. J. Neurosci. Res. 90 (4), 743–750.

Farina, M., Campos, F., Vendrell, I., Berenguer, J., Barzi, M., Pons, S., Suñol, C., 2009. Probucol increases glutathione peroxidase-1 activity and displays long-lasting protection against methylmercury toxicity in cerebellar granule cells. Toxicol. Sci. 112, 416–426.

Farina, M., Aschner, M., Rocha, J., 2011. Oxidative stress in MeHg-induced neurotoxicity. Toxicol. Appl. Pharm. 256, 405–417.

Fonfría, E., Rodríguez-Farré, E., Suñol, C., 2001. Mercury interaction with the GABAA receptor modulates the benzodiazepine binding site in primary cultures of cerebellar granule cells. Neuropharmacology 41, 819–833.

Fonfría, E., Vilaró, M.T., Babot, Z., Rodríguez-Farré, E., Suñol, C., 2005. Mercury compounds disrupt neuronal glutamate transport in cultured mouse cerebellar granule cells. J. Neurosci. Res. 79, 545–553.

Fujimura, M., Usuki, F., Sawada, M., Rostene, W., Godefroy, D., Takashima, A., 2009. Methylmercury exposure downregulates the expression of Racl and leads to neuritic degeneration and ultimately apoptosis in cerebrocortical neurons. Neurotoxicology 30, 16–22.

Gassó, S., Cristòfol, R.M., Selema, G., Rosa, R., Rodríguez-Farré, E., Sanfeliu, C., 2001. Antioxidant compounds and Ca(2+) pathway blockers differentially protect against methylmercury and mercuric chloride neurotoxicity. J. Neurosci. Res. 66, 135–145.

Gourlay, C.W., Ayscough, K.R., 2005. The actin cytoskeleton: a key regulator of apoptosis and ageing? Nat. Rev. Mol. Cell Biol. 2, 583–589.

Hogberg, H.T., Kinsner-Ovaskainen, A., Coecke, S., Hartung, T., Bal-Price, A.K., 2010. mRNA expression is a relevant tool to identify developmental neurotoxicants using an in vitro approach. Toxicol. Sci. 113, 95–115.

Khan, M.A., Wang, F., 2009. Mercury-selenium compounds and their toxicological significance: toward a molecular understanding of the mercuryselenium antagonism. Environ. Toxicol. Chem. 28, 1567–1577.

Klamt, F., Zdanov, S., Levine, R.L., Pariser, A., Zhang, Y., Zhang, B., Yu, L.-R., Veenstra, T. D., Shacter, E., 2009. Oxidant-induced apoptosis is mediated by oxidation of the actin-regulatory protein cofilin. Nat. Cell Biol. 11, 1241–1248.

Korogi, Y., Takahashi, M., Shinzato, J., Okajima, T., 1994. MR findings in seven patients with organic mercury poisoning (Minamata disease). Am. J. Neuroradiol. 15 (8), 1575–1578.

Li, J., Li, Q., Xie, C., Zhou, H., Wang, Y., Zhang, N., Shao, H., Chan, S.C., Peng, X., Lin, S.C., Han, J., 2004. Beta-actin is required for mitochondria clustering and ROS generation in TNF-induced, caspase-independent cell death. J. Cell Sci. 117, 4673–4680.

Li, G., Cheng, Q., Liu, L., Zhou, T., Shan, C., Hu, X., Zhou, J., Liu, E., Li, P., Gao, N., 2013. Mitochondrial translocation of cofilin is required for allyl isothiocyanate-mediated cell death via ROCK1/PTEN/PI3 K signaling pathway. Cell Commun. Signal. 11, 50.

Li, S., Xu, S., Roelofs, B.A., Boyman, L., Lederer, W.J., Sesaki, H., Karbowski, M., 2015a. Transient assembly of F-actin on the outer mitochondrial membrane contributes to mitochondrial fission. J. Cell Biol. 208 (1), 109–123.

Li, G., Zhou, J., Budhraja, A., Hu, X., Chen, Y., Cheng, Q., Liu, L., Zhou, T., Li, P., Liu, E., Gao, N., 2015b. Mitochondrial translocation and interaction of cofilin and Drp1 are required for erucin-induced mitochondrial fission and apoptosis. Oncotarget 6 (3), 1834–1849.

Livak, K.J., Schmittgen, T.D., 2001. Analysis of relative gene expression data using realtime quantitative PCR and the $2^{-\Delta\Delta C_T}$ method. Methods 25, 402–408.

Mergler, D., Anderson, H.A., Chan, L.H., Mahaffey, K.R., Murray, M., Sakamoto, M., Stern, A.H., 2007. Panel on Health Risks and Toxicological Effects of Methylmercury. Methylmercury exposure and health effects in humans: a worldwide concern. Ambio 36 (1), 3–11.

Miura, K., Kobayashi, Y., Toyoda, H., Imura, N., 1998. Methylmercury-induced microtubule depolymerization leads to inhibition of tubulin synthesis. J. Toxicol. Sci. 23 (5), 379–388.

Mizuno, K., 2013. Signaling mechanisms and functional roles of cofilin phosphorylation and dephosphorylation. Cell. Signal. 25, 457–469.

O'Kusky, J., 1983. Methylmercury poisoning of the developing nervous system: morphological changes in neuronal mitochondria. Acta Neuropathol. 61, 116–122.

Olguín, N., Champomier-Verges, M., Anglade, P., Baraige, F., Cordero-Otero, R., Bordons, A., Zagorec, M., Reguant, C., 2015. Transcriptomic and proteomic analysis of Oenococcus oeni PSU-1 response to ethanol shock. Food Microbiol. 51, 87–95.

Pfaffl, M.W., Tichopad, A., Prgomet, C., Neuvians, T.P., 2004. Determination of stable housekeeping genes, differentially regulated target genes and sample integrity: BestKeeper – excel-based tool using pair-wise correlations. Biotechnol. Lett. 26, 509–515.

Popova, D., Jacobsson, S.O.P., 2014. A fluorescence microplate screen assay for the detection of neurite outgrowth and neurotoxicity using an antibody against bIII-tubulin. Toxicol. In Vitro 28, 411–418.

Ramon, R., Murcia, M., Aguinagalde, X., Amurrio, A., Llop, S., Ibarluzea, J., Lertxundi, A., Alvarez-Pedrerol, M., Casas, M., Vioque, J., Sunyer, J., Tardon, A., Martinez-Arguelles, B., Ballester, F., 2011. Prenatal mercury exposure in a multicenter cohort study in Spain. Environ. Int. 37, 597–604.

Regueiro, J., Olguín, N., Simal-Gándara, J., Suñol, C., 2015. Toxicity evaluation of new agricultural fungicides in primary cultured cortical neurons. Environ. Res. 140, 37–44.

Rehklau, K., Gurniak, C.B., Conrad, M., Friauf, E., Ott, M., Rust, M.B., 2012. ADF/cofilin proteins translocate to mitochondria during apoptosis but are not generally required for cell death signaling. Cell Death Differ. 19, 958–967.

Sakamoto, M., Yasutake, A., Domingo, J.L., Chan, H.M., Kubota, M., Murata, K., 2013. Relationships between trace element concentrations in chorionic tissue of placenta and umbilical cord tissue: potential use as indicators for prenatal exposure. Environ. Int. 60, 106–111.

Samstag, Y., John, I., Wabnitz, G.H., 2013. Cofilin: a redox sensitive mediator of actin dynamics during T-cell activation and migration. Immunol. Rev. 256, 30–47.

Sanfeliu, C., Sebastia, J., Cristofol, R., Rodriguez-Farre, E., 2003. Neurotoxicity of organomercurial compounds. Neurotox. Res. 5, 283–305.

Spence, E.F., Soderling, S.H., 2015. Actin out regulation of the synaptic cytoskeleton. J. Biol. Chem. 290, 28613–28622.

Stern, M., Gierse, A., Tan, S., Bicker, G., 2014. Human Ntera2 cells as a predictive in vitro test system for developmental neurotoxicity. Arch. Toxicol. 88, 127–136.

Stringari, S., Nunes, A.K.C., Franco, J.L., Bohrer, D., Garcia, S.C., Dafre, A.L., Milatovic, D., Souza, D.O., Rocha, J.B.T., Aschner, M., Farina, M., 2008. Prenatal methylmercury exposure hampers glutathione antioxidant system ontogenesis and causes long-lasting oxidative stress in the mouse brain. Toxicol. Appl. Pharmacol. 227 (1), 147–154.

Tang, H.L., Le, A.H., Lung, H.L., 2006. The increase in mitochondrial association with actin precedes Bax translocation in apoptosis. Biochem. J. 396, 1–5.

Utsumi, T., Sakurai, N., Nakano, K., Ishisaka, R., 2003. C-terminal 15 kDa fragment of cytoskeletal actin is posttranslationally N-myristoylated upon caspase-mediated cleavage and targeted to mitochondria. FEBS Lett. 539, 37–44.

Vendrell, I., Carrascal, M., Vilaro, M.T., Abian, J., Rodriguez-Farre, E., Suñol, C., 2007. Cell viability and proteomic analysis in cultured neurons exposed to methylmercury. Hum. Exp. Toxicol. 26, 263–272.

Vendrell, I., Carrascal, M., Campos, F., Abian, J., Suñol, C., 2010. Methylmercury disrupts the balance between phosphorylated and nonphosphorylated cofilin in primary cultures of mice cerebellar granule cells. A proteomic study. Toxicol. Appl. Pharmacol. 242, 109–118.

Vieira, H.C., Morgado, F., Soares, A.M.V.M., Abreu, S.N., 2015. Fish consumption recommendations to conform to current advice in regard to mercury intake. Environ. Sci. Pollut. Res. 22, 9595–9602.

WHO. World Health Organization, 2007. Exposure to mercury: a major public health concern. . http://www.who.int/phe/news/Mercury-flyer.pdf.

Wang, C., Zhou, G.L., Vedantam, S., Li, P., Field, J., 2008. Mitochondrial shuttling of CAP1 promotes actin- and cofilin-dependent apoptosis. J. Cell Sci. 121, 2913–2920.

Wolf, M.B., Baynes, J.W., 2007. Cadmium and mercury cause an oxidative stress-induced endothelial dysfunction. Biometals 20, 73–81.

Xu, X., Newman, M.C., 2015. Exposure as a function of fish consumption in two Asian communities in Coastal Virginia, USA. Arch. Environ. Contam. Toxicol. 68, 462–475.

Yoshino, Y., Mozai, T., Nakao, K., 1966. Biochemical changes in the brain in rats poisoned with an alkymercury compound: with special reference to the inhibition of protein synthesis in brain cortex slices. J. Neurochem. 13, 1223–1230.

Zdanov, S., Klamt, F., Shacter, E., 2010. Importance of cofilin oxidation for oxidant-induced apoptosis. Cell Cycle 9, 1675–1677.

Zhang, P., Xu, Y., Sun, J., Li, X., Wang, L., Jin, L., 2009. Protection of pyrroloquinoline quinone against methylmercury-induced neurotoxicity via reducing oxidative stress. Free Radic. Res. 43, 224–233.